DOI: 10.1002/chem.200700233

Synthesis and Heavy-Metal-Ion Sorption of Pure Sulfophenylenediamine Copolymer Nanoparticles with Intrinsic Conductivity and Stability

Qiu-Feng Lü, Mei-Rong Huang,* and Xin-Gui Li*[a]

Abstract: Novel copolymer nanoparticles were easily synthesized with a polymerization yield of 59.3% by an oxidative precipitation polymerization of aniline (AN) and *m*-sulfophenylenediamine (SP) in HCl without any external stabilizer. The polymerization yield, size, morphology, electroconductivity, solubility, solvatochromism, lead and mercury ion adsorbability of the HCl-doped copolymer salt particles were studied by changing the AN/SP ratio. The AN/SP (80:20) copolymer particles are found to have the minimal number-average diameter(84.4 nm), minimal size polydispersity index (1.149), high stability, good long-term stability, powerful redispersibility in water, high purity, and clean surface because of a complete elimination of the contamination from external stabilizer. The copolymer salts possess a remarkably enhanced solubility, interesting solvatochromism, and widely adjustable electroconductivity moving across nine orders of magnitudes from 10^{-9} to 10^{0} S cm^{-1}. The AN/SP (70:30) copolymer particles have the highest Hg^{2+} adsorbance and adsorptivity of 497.7 mg g^{-1} and 98.8%, respectively, which are much higher values than those of other materials. The sorption mechanism of lead and mercury ions on the particles is proposed. The copolymer bases with 5–10 mol% SP unit show excellent film formability, flexibility, and smooth appearance. The copolymer should be very useful in the fabrication of cost-effective conductive nanocomposite with low percolation threshold and in removal of toxic metallic ions from waste water.

Keywords: conducting materials · copolymerization · nanocomposite · nanotechnology · polyaniline

Introduction

Nanostructured conducting polymers have received great attention because of their attractive electronic, optical, magnetic, reactive, and catalytic properties associated with their nanometer- or quantum-scale dimensions.[1–5] Polyaniline (PAN) is one of the most promising conducting polymers for its electronic, electrochemical, electrorheological and optical properties, good environmental and thermal stability,[6] and applications including catalyst,[7] light emitting diodes,[8] sensors,[9,10] gas separation membranes,[11] and electrorheological fluids.[12,13] However, the practical exploitation of PAN has been hampered to some extent because of its intractable nature, that is, its infusibility at melt processing temperature and poor solubility in common solvents except for H_2SO_4 and *N*-methylpyrrolidone (NMP). An attractive approach to efficiently improve its processibility is to prepare nano-sized particles. Emulsion,[14] miniemulsion,[15] and inverted emulsion[16] polymerizations have been used for the successful generation of PAN nanoparticles. PAN colloid dispersions can be produced by chemical oxidative polymerization of aniline (AN) in the presence of micelles,[17–19] or steric stabilizers, such as poly(vinyl alcohol),[20] poly(*N*-vinylpyrrolidone),[21] amphiphilic polymer surfactant,[22] and ethyl(hydroxyethyl) cellulose.[23] The pulsed potentiostatic method has also been applied to prepare the PAN nanoparticles on a highly oriented pyrolytic graphite surface by electrochemical polymerization.[24] Unfortunately, these traditional polymerization methods usually lead to complicated synthetic conditions that require the removal of external emulsifier or stabilizer and produce lower yield with poorer reproducibility.[25] Furthermore, the size, morphology, and stability of PAN particles prepared by dispersion polymerization are strongly dependent on the choice of stabilizer, oxidant, and reaction conditions.[19] Electrochemical polymerization can produce nanoparticles without using an emulsifier or stabilizer, but the nanoparticles can only be made on a limited scale. Recently, a strategy for simply preparing the

[a] Dr. Q.-F. Lü, Prof. M.-R. Huang, Prof. Dr. X.-G. Li
Institute of Materials Chemistry
Key Laboratory of Advanced Civil Engineering Materials
College of Materials Science and Engineering, Tongji University
1239 Siping Road, Shanghai 200092 (China)
Fax: (+86) 21-6598-0524
E-mail: huangmeirong@tongji.edu.cn
adamxgli@yahoo.com

conducting particles based on poly(1,8-diaminonaphthalene-*co*-4-sulfonic diphenylamine)[26] and poly(8-aminoquinoline-*co*-2-ethylaniline)[27] without using any external emulsifier or stabilizer has been proposed because the comonomer units containing charged groups could also be served as internal stabilizer. Furthermore, the HCl-doped AN copolymer nanoparticles obtained thus possess strong redispersibility and high stability in aqueous or organic media and also high conductivity.[28]

The polymers from the AN derivatives, which bear various functional groups, exhibit some unique properties; especially polymers from phenylenediamine.[6] The polymers of three isomers of *o*-, *m*-, and *p*-phenylenediamines have become an important subject of active investigation because of their better performances of reversible redox reactivity, complexability, electroactivity, gas permselectivity, and electrochromism and their promising applications, such as electrocatalyst, electronic materials, sensors, detectors, and heavy metal-ion sorbent.[6] For heavy metal-ion sorption, the aromatic amine polymers generally possess stronger adsorbability, faster adsorption rate, and lower costs than traditional adsorbents such as the activated carbon and chelate resin.[26] Therefore, the aromatic amine polymers would be very useful because lead and mercury are fairly widespread in our consumer society[28] and probably the most serious toxic metals with cumulative and nondegradative nature.

The purpose of this article is to demonstrate simple preparation methods for narrow-distributed conducting copolymer nanoparticles from AN and *m*-sulfophenylenediamine (SP) monomers based on the classic chemical oxidative polymerization. This would be particularly important because the presence of negatively charged sulfonic groups could significantly change the formation and stability of the copolymer particles owing to their interchain electrostatic repulsion,[28] thus leading to an in situ fabrication of pure stable nanoparticles. The effect of AN/SP ratio on the number-average diameter and size polydispersity index, morphology, solubility, solvatochromism, electrical conductivity, heavy metal ions adsorbability, and film formability of the copolymers was systematically investigated. Furthermore, the nanocomposite film of PANSP (80:20) copolymer nanoparticles in methyl cellulose was also reported.

Results and Discussion

Synthesis of the PANSP copolymer nanoparticles: The chemical oxidative copolymerization of AN and SP monomers with ammonium peroxydisulfate as an oxidant in 1.0 M HCl aqueous solution at 25 °C affords fine and uniform dark green or black particles as products. The progress in the copolymerization was followed by measuring the reaction solution temperature. It was found that with dropping oxidant solution slowly and regularly, the polymerization solution temperature increased first and then decreased, and finally reached a nearly constant temperature. With increasing SP content from 0 to 90 mol %, the exothermic capacity from the copolymerization steadily decreases, that is, both the maximum temperature and the enhanced solution temperature decrease. AN/SP (100:0) polymerization, having an enhancement of the solution temperature of 4.6 °C, exhibits the strongest exothermic capability among the seven AN/SP copolymerization systems, indicating the strongest polymerizing tendency and the most violent polymerization. On the contrary, AN/SP (10:90) copolymerization exhibits the weakest exothermic effect with an enhancement of the solution temperature of 0.8 °C. These results suggest that the exothermic capacity from the polymerization is significantly dependent on the AN/SP ratio. That is to say, the chain propagation by adding SP units becomes slower as the SP monomer content increases because of the electron withdrawing and great steric effects of sulfonic group on phenyl ring.

As shown in Figure 1, the polymerization yield dramatically increases from 18.7 to 90.0 % with increasing AN content from zero to 100 %, which may be owing to the activation of SP polymerizability by AN monomer and also loss of less water-soluble oligomers during the washing step. As mentioned above, the steric hindrance and attracting electron effect from $-SO_3H$ could deactivate or weaken the polymerizability of SP monomer. Maybe it is difficult for one SP unit to interlink another SP unit during the polymerization, but it is easier for the SP unit to interlink AN unit. That is to say, the presence of AN monomer would activate or enhance the chemical oxidative polymerization of SP monomer. Therefore, it could be speculated that the PANSP copolymer synthesized here would be random. A basically similar variation of the yield with 4-sulfonic diphenylamine content was found for 4-sulfonic diphenylamine/aniline copolymers.[28] Note that novel AN/SP (80:20) copolymer nanoparticles possessing the minimal number-average diameter and size polydispersity index of 84.4 nm and 1.149 respectively were facilely synthesized with a polymerization yield of 59.3 %, as discussed below. In particular, the preparation of the nanoparticles in HCl without any external stabilizer is very cost effective because of high monomer concentration (2.3 wt %), relatively high yield (59.3 %), strong stability/long-term stability/redispersibility, high purity, and clean surface of the nanoparticles as compared with low AN

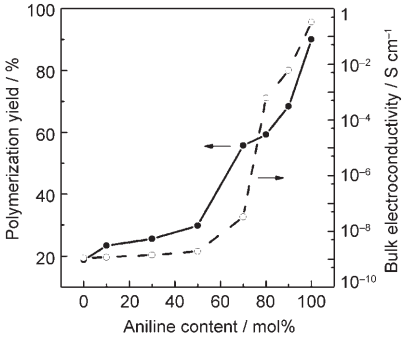

Figure 1. Variation of the polymerization yield and bulk electrical conductivity of the HCl-doped PANSP copolymer salts with the AN content.

monomer concentration (0.1–0.5 wt%) used for traditional miniemulsion polymerization as well as low yield (6–10%) of PAN nanomaterials.[10]

Structures of the PANSP copolymer nanoparticles

IR Spectra: The IR spectra for the HCl-doped copolymer salts with eight AN/SP ratios are shown in Figure 2. A broad absorption band at 3440–3312 cm^{-1} can be described to N–H stretching vibration,[28,29] which suggests the presence of secondary amino groups in the polymers. Note that the N–H stretching band at 3440–3312 cm^{-1} seems to disappear for 90:10 and 80:20 PAN/SP polymers,[26] possibly due to an interaction between the -NH- and sulfonic groups. Reappearance of stronger N-H stretching band for the polymers with 30–100 mol% SP unit could be attributable to 1) the introduction of twice more -NH- groups than sulfonic group because each SP unit contains one sulfonic group but two amino groups; 2) lower molecular mass for the polymers with more SP unit, which has been confirmed by much lower conductivity (Figure 1) and shorter conjugated length (see Figures 3 and 8 and Table 1). The two absorptions at 1621–1554 and 1521–1480 cm^{-1} are associated with the stretching of quinoid and benzenoid rings, respectively. A medium peak at 1309–1294 cm^{-1} should be due to C–N stretching vibration in an alternative unit of quinoid–benzenoid–quinoid and becomes weaker with adding SP unit. A shoulder peak at 1217–1234 cm^{-1} is ascribed to the C–N stretching in the benzenoid–benzenoid–benzenoid triad sequence.[29b] The strong absorption at 1067–1052 cm^{-1} is related to the asymmetric stretching vibration of the S=O group. The band at 1021–1015 cm^{-1} should be attributable to S=O symmetric stretching of the $-SO_3^-$ group on the SP unit,[28] because the band intensity increases significantly as SP content rises. The peaks at 709 and 620 cm^{-1} are owing to the stretching vibration of C–S and S–O bonds on the SP unit, respectively. Especially, the peak at 1021–1015 cm^{-1} is present in seven SP unit containing polymers, but is absent from the PAN spectrum. Moreover, the homopolymer of SP monomer is totally soluble in water. These results signify that the copolymers obtained are the real copolymers, rather than the mixture of AN and SP homopolymers.

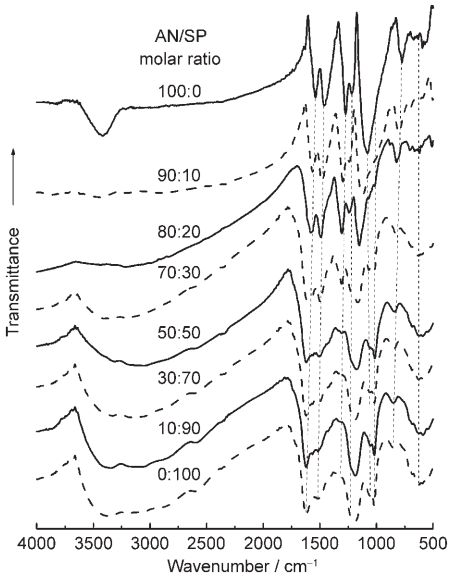

Figure 2. IR spectra of the HCl-doped copolymer salts with different AN/SP molar ratios.

UV/vis Spectra: As shown in Figure 3, the UV/Vis absorption spectra of all eight HCl-doped polymer salts in DMSO exhibit two absorption bands, the first band at 330–326 nm assigned to π–π* transition of the benzenoid ring,[28] and the second band around 630–552 nm assigned to n–π* excitation of benzenoid to the quinoid ring in the polymer chain. It is observed that the exciton band experiences a hypsochromic shift with increasing SP content from 0 to 100%, implying a decreased conjugation extent and an increased band gap. The blue shift with increasing SP content is presumably due to the steric repulsion between the sulfonic group and the hydrogen on the adjacent phenyl rings,[29] producing torsional twists and therefore shortening the conjugation lengths.

X-ray Diffractograms: The wide-angle X-ray diffractograms for virgin HCl-doped particles of the PANSP polymers in Figure 4 suggest that the particles are substantially amorphous. The PAN shows four diffraction peaks at the Bragg

Table 1. The effect of AN/SP ratios on the solubility and solvatochromism of the HCl-doped PANSP copolymers with $(NH_4)_2S_2O_8$/monomer molar ratio of 1/1 in 1.0 M HCl at 25 °C for 24 h.

AN/SP molar ratio	Solubility[a] (solution color,[b] UV/Vis maximal absorption wavelength (nm))						
	NMP	Formic acid	DMF	DMSO	NH_4OH	Water	THF
Polarity index	6.7	20[c]	6.4	6.5	–	10	4.2
100:0	S(b,637)	MS(g,825)	MS(b)	PS(b,629)	IS	IS	IS
90:10	MS(b)	MS(b,818)	MS(b)	MS(b,621)	IS	IS	IS
80:20	MS(b)	MS(br,540)	MS(bg)	MS(br,618)	MS(br)	IS	IS
70:30	SS(o)	MS(br,524)	MS(br)	S(br,554)	S(br)	SS(o)	IS
50:50	SS(o)	MS(br,522)	MS(br)	S(br,552)	S(br)	PS(o)	IS
30:70	SS(o)	MS(br,514)	MS(o)	S(br,540)	S(br)	PS(o)	IS
10:90	SS(o)	MS(br)	MS(o)	S(br)	S(br)	MS(br)	IS
0:100	SS(o)	MS(br)	MS(o)	S(br)	S(br)	S(br)	IS

[a] Solubility: IS = insoluble, MS = mainly soluble, PS = partially soluble, S = soluble, SS = slightly soluble. [b] Solution color: b = blue, bg = bluish green, br = brown, g = green, o = orange. [c] An estimated value based on the polarity index and dielectric constant of acetic acid.

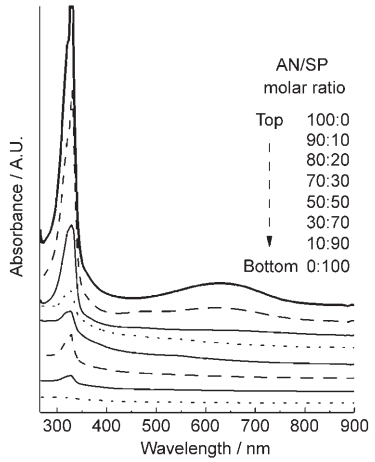

Figure 3. UV/Vis absorption spectra of the copolymer salts with different AN/SP molar ratios in DMSO at 10 mg L^{-1}.

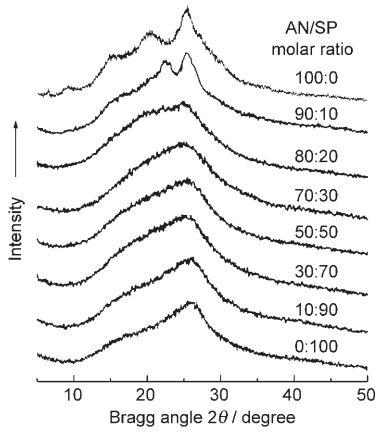

Figure 4. X-ray diffraction patterns for the HCl-doped copolymer salts with AN/SP molar ratios of 100:0, 90:10, 80:20, 70:30, 50:50, 30:70, 10:90 and 0:100.

angle 2θ of 9.3, 15.0, 20.3 and 25.3°. The two strongest peaks centered at 20.3 and 25.3° should be ascribed to the periodicity parallel and perpendicular to the polymer chains.[30] For the PANSP (90:10) copolymer, the pattern exhibits two peaks at 22.5 and 25.3°. With increasing the SP content from 20 to 100 mol%, the peaks gradually merge one peak at 25.3°. It seems that the polymers containing 30–70 mol% SP units have the highest amorphousness because they exhibit only one broad diffraction peak. The polymers containing 90–100 mol% SP units display one major diffraction peak at 25.3° and a weak shoulder peak at 17°. In addition, it should be noticed that the PAN has a peak centered at 20.3° that is assigned to a repeating unit of PAN molecular chain, while this peak disappears or merges in PANSP polymers. The disappearance or mergence may be an indication that the product is a copolymer rather than a mixture of two homopolymers.

Size and morphology of the PANSP copolymer nanoparticles: It is seen from Figure 5 that the number-average diameter (D_n) and size polydispersity index (PDI = weight-average diameter (D_w)/D_n) of the HCl-doped PANSP copolymer particles analyzed by LPA exhibit a significant dependency on the SP content. The D_n and PDI significantly decrease first and then increase with increasing AN content from 0 to 100%, exhibiting the D_n and PDI of 84.4 nm and 1.149, respectively, at the AN content of 80 mol%. The decrease of the particle diameters with increasing AN content should be attributed to gradually weakened water-swelling effect of sulfonic groups on less SP units. The minimal D_n and PDI might be ascribed to the weakest water-swelling effect and strongest static repulsion of the negatively charged sulfonic groups on the SP units, which can efficiently stabilize as-formed nanoparticles. However, the PANSP polymers containing 90–100 mol% AN units exhibit larger D_n than the PANSP (80:20) copolymer, possibly due to weaker static repulsion of as-formed particles containing less sulfonic groups of the former than the latter. Particularly, the PANSP (80:20) copolymer nanoparticles have not only high stability but also good long-term stability in water. After the nanoparticles have been stored in water for one year, their D_n and PDI increase slightly from 84.4 nm and 1.149 to 102 nm and 1.170, respectively.

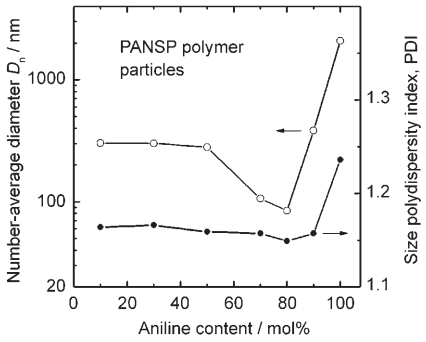

Figure 5. Variation of the number-average diameter (D_n) and size polydispersity index (PDI = D_w/D_n) of the HCl-doped PANSP copolymer particles with AN content synthesized with $(NH_4)_2S_2O_8$/monomer molar ratio of 1:1 in 1.0 M HCl at 25 °C for 24 h.

The nanoparticles of the HCl-doped PANSP (80:20) copolymer were further analyzed by AFM and TEM observations, as shown in Figure 6. The AFM and TEM images show that the nanoparticles appear to be ellipsoidal rather than spherical. In Figure 6a, the nanoparticles exhibit a statistically mean diameter of 80.2 nm, which was in good agreement with the result determined by laser particle analyzer. The TEM image in Figure 6b shows that the copolymer nanoparticles exhibit a mean diameter of 75 nm in a diameter range from 48 to 97 nm. This signifies that the copolymer nanoparticles synthesized in this way exhibit narrow distribution. The size of the nanoparticles revealed by TEM is smaller than that by laser particle analyzer and AFM because of much stronger shrinkage of nanoparticles resulting

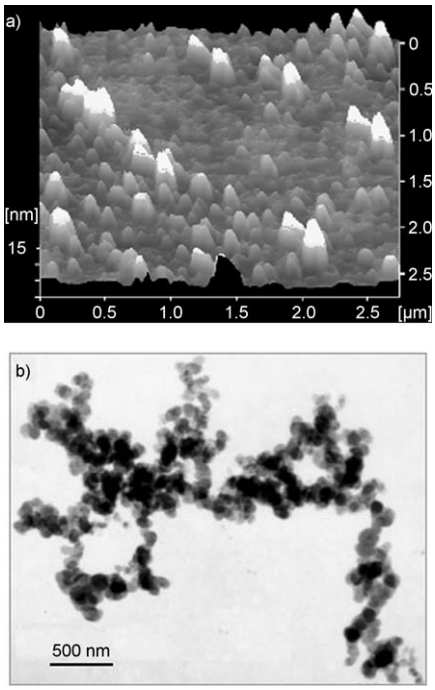

Figure 6. a) AFM and b) TEM images of the nanoparticles of HCl-doped PANSP (80:20) copolymer salt.

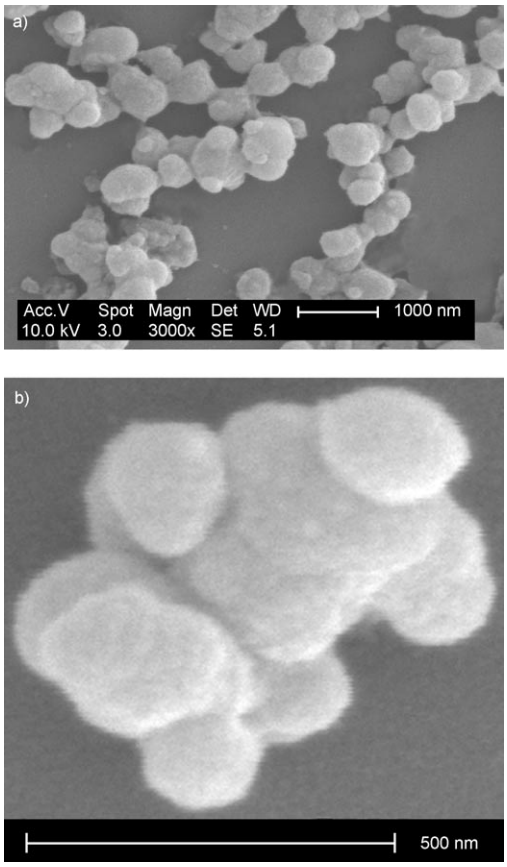

Figure 7. FE-SEM images of the HCl-doped PANDPS (50:50) copolymer salt particles.

from larger loss of absorbed water in a high vacuum during TEM measurement.

The particles of the HCl-doped PANSP (50:50) copolymer show mean diameter of 280 nm by a laser particle analyzer in Figure 5, which is much larger than that of the HCl-doped PANSP (80:20) copolymer nanoparticles. The PANSP (50:50) copolymer particles were also investigated by FE-SEM observation, as shown in Figure 7. The FE-SEM images show that the particles are ellipsoidal and have a mean diameter of 270 nm in a diameter range from 100 to 340 nm. These agree basically with those revealed by LPA measurement.

Apparently, the existence of sulfonic side groups on the copolymers permits the particle size to be easily controlled and regulated by varying the SP content because the sulfonic group as an internal stabilizer can provide strong static repulsion amongst the particles and efficiently stabilize the nanoparticles. Therefore, the nanoparticles obtained here have high purity and clean surface because 1) no external stabilizer or dispersant was added into the polymerization medium and 2) dissociative HCl, residual AN/SP monomers and $(NH_4)_2S_2O_8$, and its reducing product $(NH_4)_2SO_4$ in/on the nanoparticles have been totally removed by centrifugation in water.

It is noted from Figure 5 that the D_n and PDI of the copolymer particles are non-monotonically dependent on the SP content because of a strong copolymerization effect between the monomers. It is concluded that the AN/SP molar ratio of 80:20 is optimal for the facile synthesis of the copolymer nanoparticles with an intrinsic stability in liquid media.

Properties of the PANSP copolymer nanoparticles

Solubility: The solubility and solution color of the HCl-doped PANSP copolymers in various solvents are listed in Table 1. There is no solvent in which all PANSP polymers are completely soluble. It seems difficult to examine the molecular weight of the polymers in the same solvent. The solubility and solution color of the PANSP polymers drastically depend on the AN/SP ratio and solvents used. All polymers are mainly soluble in formic acid and DMF. It is interesting that the copolymers show a gradually enhanced solubility in DMSO, NH_4OH and water with increasing SP content, but a gradually weakened solubility in NMP. Obviously, the PANSP (80:20) copolymer has an enhanced solubility compared with polyaniline, that is, PANSP (100:0). The variation of the copolymer solubility with SP content is a reflection of various macromolecular structures. The remarkably enhanced solubility of the copolymers in DMSO, NH_4OH, and water results from the incorporation of a large number of SP units in the copolymer chains and amorphous supramolecular structure, which enlarges the distance between the macromolecular chains and significantly diminishes interactions between the chains. Additionally, a unique dependence of solubility of the polymers in NH_4OH on the SP content indicates that the polymerization products are

indeed genuine copolymers containing the two-monomer units rather than a simple mixture of two homopolymers.

Solvatochromism: The optical absorption of polymer solution is valuable for an investigation on the change of the chain conformation induced by the interaction between the chain and the solvent. As listed in Table 1, the solution colors of the PANSP copolymer salts change with the solvents, that is, the copolymers exhibit an interesting solvatochromism that is similar to that of aminoquinoline/ethylaniline copolymers.[27] For the PANSP (80:20) copolymer, the solution colors vary from blue in NMP to brown in formic acid, DMSO and NH_4OH, and to bluish green in DMF. This indicates that the copolymer chains may have different conformations and therefore different conjugation lengths in different solvents because of diverse interactions between the polymer chains and various solvents.[30]

The solvatochromism of the copolymers with eight AN/SP ratios in DMSO and formic acid is further confirmed quantitatively by UV/Vis spectra. Their UV/Vis spectra usually have two absorption peaks in DMSO, that is, one band at 330–326 nm assigned to the π–π* transition and another band around 630–552 nm from the n–π* excitation. However, the PANSP (90:10) and PANSP (80:20) copolymers display four and three peaks, respectively, in formic acid. Noteworthy, they show strong bands at 322 nm. Furthermore, the peak intensity at 630–552 nm in DMSO in Figure 3 and at 825–818 nm in formic acid in Figure 8 reduces with increasing the SP content. As listed in Table 1, the UV/Vis maximal absorption wavelength of the excitation bands around 825 nm in formic acid and 634 nm in DMSO exhibits a hypsochromic shift with elevating SP content from 0 to 100 mol%, implying that the conjugated length of the copolymers is slowly shortened. The interesting strong solvatochromism should be attributed to the variations of doping level, conjugating extent, polymer nature, and polymer-solvent interaction with solvent nature. The solvatochromism might originate from the electron transfer between the solvent molecules and the imino groups of the solvated polymer.[31,32] This electron transfer will raise the electron density of the imine nitrogen and the dipole moment directed toward the nitrogen atom, consequently lowering the energy of the ground state.

Bulk electroconductivity: As shown in Figure 1, the bulk electrical conductivity of the pressed pellets of virgin HCl-doped PANSP copolymers is powerfully related to the SP content. The conductivity increases first from 1.08×10^{-9} to $6.11\times10^{-4}\,S\,cm^{-1}$, then increases rapidly to $0.329\,S\,cm^{-1}$ with increasing AN content from zero to 80 and 100%. Apparently, lower conductivity of the copolymer containing more SP units is due to the existence of the more sulfonic side groups inducing the steric effect and torsional twists in the polymer backbone, which decreases its coplanarity, and brings on a barrier to the intrachain transfer and interchain jumping of the electrons, thereby shortening the conjugation length.[28,33] This result has been verified by the UV/Vis data in Table 1 and Figures 3 and 7. It is seen that a widely variable electrical conductivity moving across nine orders of magnitudes between 10^{-9} and $10^{0}\,S\,cm^{-1}$ (Figure 1) could be simply realized for the PANSP copolymer. In other words, the polymer conductivity is facilely adjustable in a range of nine orders of magnitude, as expected.

Lead- and mercury-ion sorption: As shown in Figure 9, the Pb^{2+} adsorbance and adsorptivity onto the PANSP copolymer particles at initial Pb^{2+} concentrations of 1 and 5 mM for the adsorption time of 6 h increase first and then decrease with increasing AN content from 70 to 100 mol%. Actually, the PANSP (95:5) copolymer particles possess the maximal adsorbance and adsorptivity at any initial Pb^{2+} concentration. With increasing initial Pb^{2+} concentration from 1 to 5 mM, the Pb^{2+} adsorbance onto the PANSP (95:5) copolymer particles increases from 71.6 to $161.6\,mg\,g^{-1}$, while corresponding adsorptivity decreases from 70.6 to 31.2%, since the introduction of a small amount of sulfonic groups results in an increased distance between the copolymer chains to some extent. However, the

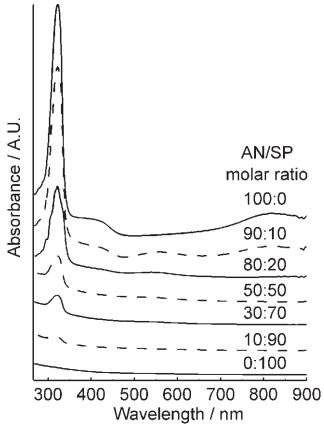

Figure 8. UV/Vis absorption spectra of the HCl-doped copolymers with different AN/SP molar ratios in formic acid at the concentration of $10\,mg\,L^{-1}$.

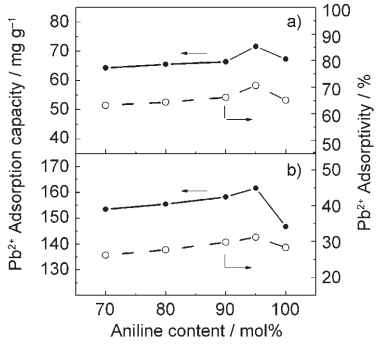

Figure 9. Variation of adsorption capacity and adsorptivity of Pb^{2+} for the HCl-doped PANSP copolymer salts with different AN contents in 25 mL $Pb(NO_3)_2$ solution at initial Pb^{2+} concentration of a) 1 mM and b) 5 mM at 30°C for 6 h.

incorporation of more than 5 mol% polar sulfonic groups might strengthen the interaction and thus shorten the distance between the chains. Gradually increased solubility of the particles in $Pb(NO_3)_2$ aqueous solution could be another reason why the Pb^{2+} adsorbability reduces slightly with increasing SP content from 5 to 30 mol%.

PANSP copolymer particles exhibit different adsorption behavior in initial Hg^{2+} concentrations of 1 and 5 mM such as depicted in Figure 10. The PANSP particles adsorb Hg^{2+}

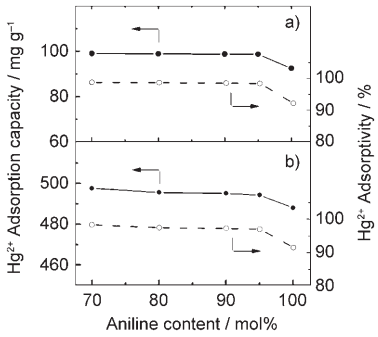

Figure 10. Variation of adsorption capacity and adsorptivity of Hg^{2+} onto the HCl-doped PANSP copolymer salts with different AN contents in 25 mL $Hg(NO_3)_2$ solution at initial Hg^{2+} concentrations of a) 1 mM and b) 5 mM at 30°C for 24 h.

more efficiently than Pb^{2+} at the same ion concentration. Moreover, the Hg^{2+} adsorbability onto the copolymer particles remains almost constant first and then decreases with increasing AN content from 70 to 100 mol%. The PANSP (70:30) copolymer particles have the highest adsorbance of 497.7 mg g^{-1} at initial Hg^{2+} concentration of 5 mM and the highest adsorptivity of 98.8% at initial Hg^{2+} concentration of 1 mM, probably owing to the introduction of most sulfonic groups. It is interesting that all copolymer particles exhibit much higher adsorption capacity than PAN/polystyrene composite (9.15 mg g^{-1})[34] and PAN (73.2 mg g^{-1}),[35] disclosing an effective Hg^{2+} adsorption from the -N=C-/-SO_3H groups on the copolymers.

It is known that the main adsorption sites for Pb^{2+} and Hg^{2+} ions are the nitrogen atoms in the macromolecular chains because the nitrogen atom has a lone pair of electrons that can efficiently bind a metal ion to form a metal complex.[34,36] Based on the adsorption capacity shown in Figures 9 and 10, a possible adsorption mechanism of Pb^{2+} and Hg^{2+} ions onto the copolymer chains may be proposed in Figure 11. The Pb^{2+} and Hg^{2+} adsorption could be responsible for a complexation between Pb^{2+} or Hg^{2+} ions and the nitrogen atoms of the -N=C- groups through sharing their four lone pairs of electrons. However, the only -N=C- groups and/or their adjacent -SO_3H groups could act as adsorption or ion exchange sites of Hg^{2+} ions on copolymer chains, resulting in a noteworthy improvement in Hg^{2+} adsorption as compared with Pb^{2+} adsorption.

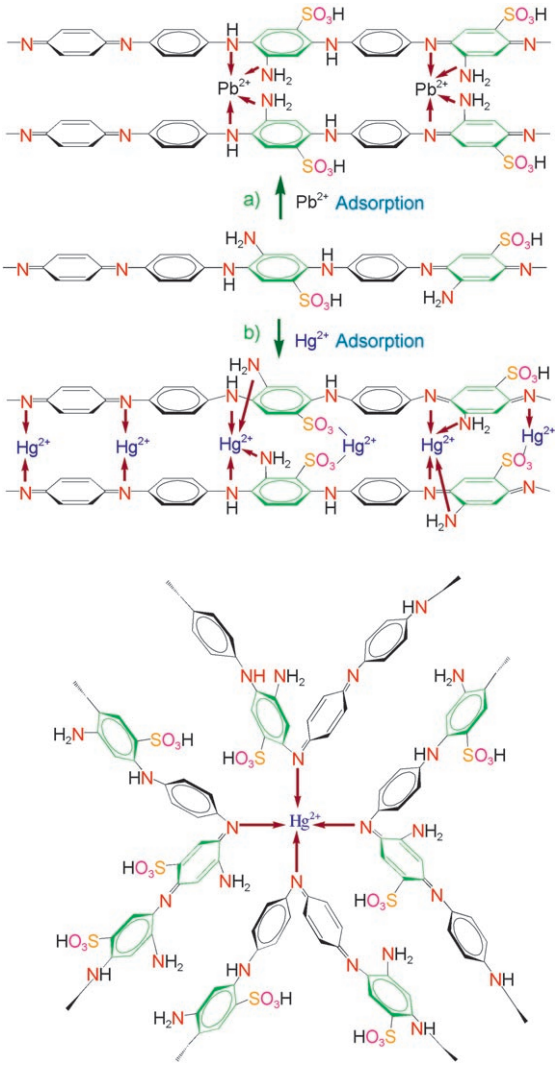

Figure 11. Possible complexations and ion exchanges between a) lead or b) mercury ions and -NH_2/-NH-/-N=C-/-SO_3H groups on the PANSP copolymer chains.

Film formability: The film-forming ability of the PANSP copolymer bases has been studied with NMP and DMSO as solvents by a solution casting method. It is seen from Table 2 that the four PANSP polymer bases in NMP solution exhibit good film formability. Furthermore, the films exhibit strong adhesion to glass and display a smooth surface without defects. In particular, the films of the PANSP (95:5) and PANSP (90:10) copolymer bases display excellent formability, flexibility and very smooth surface. Note that

Table 2. Film formability of PANSP copolymer bases in NMP at a copolymer concentration of 30 g L^{-1} at 60°C.

AN/SP molar ratio	Formability	Flexibility	Appearance
100:0	excellent	excellent	smooth, lustrous blue
95:5	excellent	excellent	very smooth, lustrous blue
90:10	excellent	excellent	very smooth, lustrous blue
80:20	good	good	smooth, dull blue

the film formability of the PANSP copolymer bases exhibits a significant dependency on the SP content. The PANSP copolymers demonstrate slightly lowered film formability and flexibility with increasing SP content from 30 to 100 mol%, because of their lowered molecular weight or increased sulfonic content.

However, the copolymer base solutions in DMSO show very poor film formability. Apparently, good solubility does not always mean good film formability. Good film formability of the bases could be ascribed to higher molecular weight and the formation of a real solution.

Conducting nanocomposite film of the copolymer nanoparticles with MC: The nanocomposite films of PANSP (80:20) copolymer nanoparticles in MC are transparent and flexible. The variation of the bulk electrical conductivity of the films at room temperature with the nanoparticle loading is shown in Figure 12. The conductivity increases from 1.02×10^{-9} to

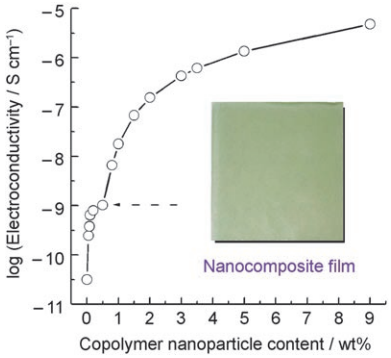

Figure 12. Effect of the nanoparticle content on bulk electroconductivity of PANSP (80:20) copolymer nanoparticles-MC nanocomposite films. The inset shows the photograph of the free-standing nanocomposite film containing 0.5 wt% nanoparticles with a thickness of 20 μm.

4.75×10^{-6} S cm^{-1} with increasing the nanoparticle content from 0.5 to 9.0 wt%. It is seen that the composite films do not show any well-defined percolation threshold. However, the data have been fitted to the scaling law of percolation theory. The method yields a percolation threshold value of 0.5 wt% and a critical exponent of 1.97, determined by linear regression analysis. The critical exponent value is in well agreement with the predicted universal value ($t=2$ for three-dimensional blend system). The percolation threshold for the PANSP (80:20) copolymer nanoparticles–MC system in this study is significantly lower than that (3.6 wt%) for the composite films from poly(3,4-ethylenedioxythiophene)/cellulose acetobutyrate.[37] The very low percolation threshold in the PANSP copolymer nanoparticle composites might be ascribed to a unique ability for the nanoparticles to tend to connect with each other and accordingly form a nanochannel or -network of effectively conducting electricity, as revealed in Figures 6band 7a. The inset in Figure 12 shows the photograph of the 20 μm-thick nanocomposite film containing 0.5 wt% of PANSP (80:20) copolymer nanoparticles. The uniform nanocomposite film is light green and exhibits excellent flexibility and conductivity of 1.02×10^{-9} S cm^{-1}.

Conclusion

Novel copolymer nanoparticles with intrinsically high stability and also good long-term stability/redispersibility in pure water or other media have been successfully synthesized by using chemical oxidative precipitation polymerization from AN and SP monomers in aqueous HCl in the absence of any external emulsifier or stabilizer. The polymerization yield, particle size, electrical conductivity, solubility and solvatochromism of the copolymers significantly depend on the comonomer ratio. It is found that the presence of sulfonic groups on the SP units permits a simple and effective fabrication of PANSP (80:20) copolymer nanoparticles as small as 48 nm with good stability, high purity, and clean surface because of a complete elimination of the contamination from external stabilizer. A non-monotonic variation of the UV/Vis spectra, X-ray diffractogram, particle size, and properties of the polymers with the AN content suggests that the polymers obtained are real copolymers rather than a simple mixture of two homopolymers. The copolymer particles are good conductor with widely adjustable conductivity moving across nine orders of magnitudes from 10^{-9} to 10^{0} S cm^{-1} by facilely regulating AN/SP ratio, as expected. The remarkably enhanced solubility in DMSO, NH_4OH, and water is observed with increasing SP content. Furthermore, the copolymer bases with 5–10 mol% of SP content exhibit excellent formability. The PANSP copolymer particles show a strong Pb^{2+} and Hg^{2+} adsorbability, indicating their potential application in recovery and elimination of harmful heavy metallic ions from waste water. The transparent, flexible and uniform nanocomposite film of the PANSP (80:20) copolymer nanoparticles–MC exhibits a low percolation threshold of 0.5 wt% because the nanoparticles possess a unique ability to link with each other and accordingly form a nano-channel or -network of efficiently conducting electricity. With increasing the nanoparticles loading from 0.5 to 9.0 wt%, the conductivity of the nanocomposite films increases from 1.02×10^{-9} to 4.75×10^{-6} S cm^{-1} that usually satisfies the requirement for antistatic materials.

Experimental Section

Reagents: Aniline (AN), *m*-sulfophenylenediamine (SP), ammonium peroxydisulfate, lead nitrate, mercury nitrate, methyl cellulose (MC), *N*-methylpyrrolidone (NMP), formic acid, dimethylformamide (DMF), dimethyl sulfoxide (DMSO), acetone, tetrahydrofuran (THF) and other solvents were commercially obtained and used as received.

Synthesis of the PANSP copolymer nanoparticles: The PANSP copolymer nanoparticles were prepared with ammonium peroxydisulfate as an oxidant in HCl aqueous solution through chemical oxidative polymerization in the absence of any external emulsifier or stabilizer. A representative polymerization for PANSP (80:20) copolymer nanoparticles was as follows (Scheme 1): AN (1.46 mL, 16 mmol) and SP (0.84 g, 4 mmol) co-

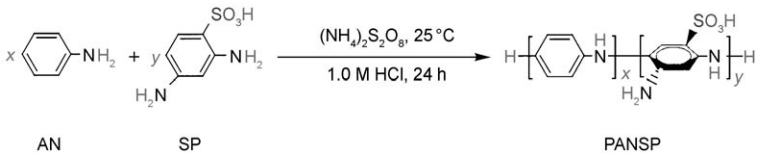

Scheme 1. Chemical oxidative copolymerization of aniline (AN) and m-sulfophenylenediamine (SP).

monomers were added to an HCl solution (1.0 M, 75 mL) in a 250 mL glass flask in water bath and stirred vigorously with an magnet stir bar for 30 min. Ammonium peroxydisulfate (4.56 g, 20 mmol) was dissolved separately in HCl (1.0 M, 25 mL) to prepare an oxidant solution. The oxidant solution was then added dropwise to the monomer solution at a rate of one drop for every 3 s at 25 °C in a period of 30 min. The reaction mixture was vigorously magnetically stirred for 24 h at 25 °C in a water bath. After the reaction, the virgin HCl-doped PANSP copolymer particles formed were isolated from the reaction mixture by filtration and washed with an excess of distilled water to remove the residual oxidant and water-soluble oligomers. The copolymer salt particles in aqueous solution were analyzed directly by laser particle-size analyzer and microscopy before drying. A dark powder was left to dry under infrared lamp for one week. The copolymer of 1.35 g was obtained with the yield of ca. 59.3 %. The resultant copolymer salt, that is, virgin doped sample, can be converted into its base, that is, dedoped sample, by dispersing the HCl-doped copolymer salt in 0.2 M NH_4OH aqueous solution with stirring for 24 h. The film formability was evaluated with NMP and DMSO as solvents at a fixed copolymer concentration (30 $g\,L^{-1}$) by a solution casting method. The solvent in copolymer solution on glass with the area of 9 × 9 cm^2 was evaporated at 60 °C.

Sorption experiments: The adsorption of Pb^{2+} and Hg^{2+} ions in aqueous solution on the copolymer particles was performed in a batch experiment. Aqueous solutions (25 mL) containing Pb^{2+} or Hg^{2+} ions at a concentration of 1 and 5 mM were incubated with a given amount of the copolymer particles at a fixed temperature of 30 °C. After a desired treatment period, the copolymer particles were filtered from the solution, and then the concentration of metal ions in the filtrate after adsorption was measured by molar titration. The adsorbed amount of Pb^{2+} and Hg^{2+} ions on the PANSP copolymer particles was calculated according to the following Equations (1) and (2):

$$Q = \frac{(c_o - c)VM}{W} \quad (1)$$

$$q = \frac{c_o - c}{c_o} \times 100\,\% \quad (2)$$

where Q is the adsorption capacity ($mg\,g^{-1}$), q is the adsorptivity (%), c_o and c are metal-ion concentrations before and after adsorption (M), respectively, V is the initial volume of the metal ions solution (mL); M is the molecular weight of metal ions ($g\,mol^{-1}$), and W is the weight of the PANSP copolymer particles added (g).

Preparation of the PANSP–MC nanocomposite films: The nanocomposite films of copolymer nanoparticles with MC were prepared by dispersing preformed PANSP (80:20) nanoparticles in MC aqueous solution and followed by solution casting onto a glass plate. After drying at 60 °C in oven for 48 h, the 15–25 μm-thick films were peeled off the glass substrates to form a freestanding sample.

Measurements: The IR spectra were recorded on a Nicolet FTIR Nexsus 470 spectrophotometer in KBr pellets. UV/Vis spectra of the polymers in DMSO and formic acid were measured on a U-3000 spectrophotometer (Hitachi Ltd, Tokyo, Japan) in a wavelength range of 190–900 nm at a scanning rate of 600 $nm\,min^{-1}$. Wide-angle X-ray diffraction scans for PANSP copolymers were obtained using a D/max 2550 X-ray model diffractometer (Rigaku, Japan) with $Cu_{K\alpha}$ radiation, at a scanned rate of 10 °min^{-1} in the reflection mode over a 2θ range from 5 to 50°. The size of the resulting PANSP copolymer particles that have been thoroughly washed with water was analyzed on Beckman Coulter LS230 laser particle-size analyzer (LPA) by using a static scattering laser with the wavelength of 750 nm. The morphologies of the PANSP copolymer particles were examined by atomic force microscopy (AFM), field-emission scanning electron microscopy (SEM, Philips XL30 FEG) and transmission electron microscopy (TEM, Hitachi Model H800), respectively. The AFM sample was prepared by dropping the aqueous solution of the copolymer particles on cover glass, and then drying in air at 25 °C. The particle samples for scanning electron microscope (SEM) observation were dispersed on glass and submitted to gold sputtering prior to the analyses. The sample for transmission electron microscope (TEM) observation was prepared by dropping the suspension of the particles on copper grids. The solubility of the copolymers was evaluated using the following method: dried polymer powders of 5 mg were added into the solvent of 1 mL and dispersed thoroughly. After the mixture was shaken continuously for 24 h at room temperature, the solubility and solution color of the polymers were characterized. The bulk electrical conductivity of a pressed pellet with the thickness of 30–40 μm for the PANSP copolymers and the nanocomposite films were measured by a two-disk method at 20 °C.[13]

Acknowledgement

The project was supported by the National Natural Science Foundation of China.

[1] A. G. MacDiarmid, *Angew. Chem.* **2001**, *113*, 2649; *Angew. Chem. Int. Ed.* **2001**, *40*, 2581.
[2] F. A. Boroumand, P. W. Fry, D. G. Lidzey, *Nano Lett.* **2005**, *5*, 67.
[3] H. Xia, D. Cheng, C. Xiao, H. S. O. Chan, *J. Mater. Chem.* **2005**, *15*, 4161.
[4] T. K. Sarma, A. Chattopadhay, *J. Phys. Chem. A* **2004**, *108*, 7837.
[5] C. M. Niemeyer, *Angew. Chem.* **2001**, *113*, 4254; *Angew. Chem. Int. Ed.* **2001**, *40*, 4128.
[6] X. G. Li, M. R. Huang, W. Duan, Y. L. Yang, *Chem. Rev.* **2002**, *102*, 2925.
[7] X. Luo, A. J. Killard, M. R. Smyth, *Chem. Eur. J.* **2007**, *13*, 2138.
[8] R. H. Friend, R. W. Gymer, A. B. Holmes, J. H. Burroughes, R. N. Marks, C. Taliani, D. D. C. Bradley, D. A. Dos Santos, J. L. Brédas, M. Lögdlund, W. R. Salaneck, *Nature* **1999**, *397*, 121.
[9] J. Janata, M. Josowicz, *Nat. Mater.* **2003**, *2*, 19.
[10] J. X. Huang, R. B. Kaner, *Angew. Chem.* **2004**, *116*, 5941; *Angew. Chem. Int. Ed.* **2004**, *43*, 5817.
[11] M. R. Anderson, B. R. Mattes, H. Reiss, R. B. Kaner, *Science* **1991**, *252*, 1412.
[12] M. S. Cho, Y. H. Cho, H. J. Choi, M. S. Jhon, *Langmuir* **2003**, *19*, 5875.
[13] M. S. Cho, H. J. Choi, K. To, *Macromol. Rapid Commun.* **1998**, *19*, 271.
[14] P. J. Kinlen, J. Liu, Y. Ding, C. R. Graham, E. E. Remsen, *Macromolecules* **1998**, *31*, 1735.
[15] E. Marie, R. Rothe, M. Antonietti, K. Landfester, *Macromolecules* **2003**, *36*, 3967.
[16] P. J. Kinlen, B. G. Frushour, Y. Ding, V. Menon, *Synth. Met.* **1999**, *101*, 758.
[17] M. G. Han, S. K. Cho, S. G. Oh, S. S. Im, *Synth. Met.* **2002**, *26*, 53.
[18] D. M. Cheng, S. C. Ng, H. S. O. Chan, *Thin Solid Films* **2005**, *477*, 19.
[19] P. A. Hassan, S. N. Sawant, N. C. Bagkar, J. V. Yakhmi, *Langmuir* **2004**, *20*, 4874.

[20] M. S. Cho, S. Y. Park, J. Y. Hwang, H. Choi, *J. Mater. Sci. Eng. C* **2004**, *24*, 15.
[21] A. Riede, M. Helmstedt, V. Riede, J. Stejskal, *Langmuir* **1998**, *14*, 6767.
[22] D. Kim, J. Choi, J. Y. Kim, Y. K. Han, D. Sohn, *Macromolecules* **2002**, *35*, 5314.
[23] D. Chattopadhyay, S. Banerjee, D. Chakravorty, B. M. Mandal, *Langmuir* **1998**, *14*, 1544.
[24] Z. Y. Tang, S. Q. Liu, Z. X. Wang, S. J. Dong, E. K. Wang, *Electrochem. Commun.* **2000**, *2*, 32.
[25] S. Virji, J. Huang, R. B. Kaner, B. H. Weiller, *Nano Lett.* **2004**, *4*, 491.
[26] X. G. Li, R. Liu, M. R. Huang, *Chem. Mater.* **2005**, *17*, 5411.
[27] X. G. Li, Y. M. Hua, M. R. Huang, *Chem. Eur. J.* **2005**, *11*, 4247.
[28] a) M. T. Nguyen, P. Kasai, J. L. Miller, A. F. Diaz, *Macromolecules* **1994**, *27*, 3625; b) X. G. Li, Q. F. Lü, M. R. Huang, *Chem. Eur. J.* **2006**, *12*, 1349; c) M. R. Huang, Q. Y. Peng, X. G. Li, *Chem. Eur. J.* **2006**, *12*, 4341.
[29] a) J. Yue, Z. H. Wang, K. R. Cromack, A. J. Epstein, A. G. MacDiarmid, *J. Am. Chem. Soc.* **1991**, *113*, 2665; b) E. T. Kang, K. G. Neoh, K. L. Tan, *Prog. Polym. Sci.* 1998, **23**, 277.
[30] J. P. Pouget, M. E. Józefowicz, A. J. Epstein, X. Tang, A. G. MacDiarmid, *Macromolecules* **1991**, *24*, 779.
[31] B. C. Roy, M. D. Gupta, L. Bhoumik, J. K. Ray, *Synth. Met.* **2002**, *130*, 27.
[32] W. Y. Zheng, K. Levon, J. Laakso, J. E. Österholm, *Macromolecules* **1994**, *27*, 7754.
[33] S. A. Chen, G. W. Hwang, *J. Am. Chem. Soc.* **1994**, *116*, 7939.
[34] R. K. Gupta, R. A. Singh, S. S. Dubey, *Sep. Purif. Technol.* **2004**, *38*, 225.
[35] R. K. Gupta, S. Shankar, *Adsorpt. Sci. Technol.* **2004**, *22*, 485.
[36] L. Jin, R. Bai, *Langmuir* **2002**, *18*, 9765.
[37] H. Randriamahazaka, F. Vidal, P. Dassonville, C. Chevrot, D. Teyssié, *Synth. Met.* **2002**, *128*, 197.

Received: February 9, 2007
Published online: May 8, 2007

